# Natural selection drives population divergence for local adaptation in a wheat pathogen

Danilo Pereira[1], Patrick C. Brunner[1]* and Bruce A. McDonald[1]*

[1] Plant Pathology Group, ETH Zurich, Universitatstrasse 2, 8092 Zurich, Switzerland.

*These authors contributed equally to this work

Corresponding author: Danilo Pereira: danilo.dossantos@usys.ethz.ch

**Abstract**

Evolution favors the emergence of locally-adapted optimum phenotypes that are likely to differ across a wide array of environmental conditions. The emergence of favorable adaptive characteristics is accelerated in agricultural pathogens due to the unique properties of agro-ecosystems. We performed a $Q_{ST}$ - $F_{ST}$ comparison using 164 strains of *Parastagonospora nodorum* sampled from eight global field populations to disentangle the predominant evolutionary forces driving population divergence in a wheat pathogen. We used digital image analysis to obtain quantitative measurements of growth rate and melanization at different temperatures and under different fungicide concentrations in a common garden experiment. $F_{ST}$ measures were based on complete genome sequences obtained for all 164 isolates. Our analyses indicated that all measured traits were under selection. Growth rates at 18°C and 24°C were under stabilizing selection ($Q_{ST} < F_{ST}$), while diversifying selection ($Q_{ST} > F_{ST}$) was the predominant evolutionary force affecting growth under fungicide and high temperature stress. Stabilizing selection ($Q_{ST} < F_{ST}$) was the predominant force affecting melanization across the different environments. Melanin production increased at 30°C but was negatively correlated with higher growth rates, consistent with a trade-off under heat stress. Our results demonstrate that global

populations of *P. nodorum* possess significant evolutionary potential to adapt to changing local conditions, including warmer temperatures and applications of fungicides.

***Keywords:*** population genetics, pathogen evolution, thermal adaptation, fungicide resistance, diversifying selection, *Parastagonospora nodorum*

## INTRODUCTION

Evolution by means of natural selection operates on individual phenotypes and is enabled by the diversity found in genes encoding quantitative traits within populations. Across a wide array of environmental conditions, evolution towards a local optimum phenotype results from the interplay among evolutionary forces such as natural selection and gene flow and stochastic events like founder events and population extinctions (Merilä & Crnokrak, 2001; Leinonen, O'Hara, Cano, & Merilä, 2008). Evolutionary processes affecting local adaptation of pathogen populations may act differently in agro-ecosystems compared to natural environments. For example, the high planting densities found in agricultural fields allow more efficient pathogen transmission and the genetic uniformity of agricultural hosts enable the development of large pathogen populations while imposing strong directional selection that accelerates the emergence of host specialization (Stukenbrock & McDonald, 2008; McDonald & Stukenbrock, 2016; Corredor-Moreno & Saunders, 2019). While particular agro-ecosystems (e.g. the one used for wheat production) tend to be highly similar on a global spatial scale, local pathogen populations can encounter significant differences in the deployment of resistant genes, pesticide exposure and annual fluctuations in temperature over a growing season (Laine, 2008;

47 Stukenbrock & McDonald, 2008; Elderd & Reilly, 2014). Hence, we expect that even globally
48 distributed pathogens can evolve different traits in different local populations according to
49 the predominating local evolutionary forces.

50 A better understanding of which evolutionary forces are driving local adaptation for
51 a particular trait can be achieved using $Q_{ST}$ - $F_{ST}$ comparisons (Zhan et al., 2005; Leinonen
52 et al., 2008; Leinonen, McCairns, O'Hara, & Merilä, 2013; Stefansson, Willi, Croll, &
53 McDonald, 2014; Yang et al., 2016). $Q_{ST}$ is an index of population differentiation based on
54 the distribution of variation for a quantitative trait (Spitze, 1993). $F_{ST}$ measures the degree
55 of population divergence based on neutral genetic markers. Natural selection is inferred
56 when population differentiation for quantitative traits is significantly different from that
57 for neutral markers ($Q_{ST} \neq F_{ST}$). Specifically, directional selection is inferred when the $Q_{ST}$ is
58 higher than the $F_{ST}$, and stabilizing selection is inferred when $Q_{ST}$ is lower than the $F_{ST}$
59 (Leinonen et al., 2013). When no differences are found between the two indexes, the
60 inference is that the trait is neutral or that it is not possible to distinguish between the
61 effects of genetic drift and natural selection in the populations being examined. Previous
62 $Q_{ST}$ - $F_{ST}$ comparisons for plant pathogenic fungi were conducted using global field
63 populations of the wheat pathogen *Zymoseptoria tritici* and the barley pathogen
64 *Rhynchosporium commune*. In both cases, natural selection was inferred to be the main
65 driver of local adaptation (Zhan et al., 2005; Stefansson et al., 2014), but directional
66 selection predominated in *Z. tritici*, while stabilizing selection was more important in *R.*
67 *commune*. These differences highlight the necessity to consider the adaptive dynamics of
68 each trait in a species-specific manner.

69 The fungal pathogen *Parastagonospora nodorum* causes stagonospora nodorum
70 blotch (SNB), a major wheat disease found around the world (Quaedvlieg et al., 2013;
71 Savary et al., 2019). Field populations of *P. nodorum* are reported to have low genetic
72 differentiation among continents, elevated population size, high genetic diversity and
73 exhibit frequent sexual recombination (Stukenbrock, Banke, & McDonald, 2006; Oliver,
74 Friesen, Faris & Solomon, 2012). SNB control measures include fungicide applications and
75 the deployment of wheat varieties that lack toxin sensitivity genes (Oliver et al., 2012;
76 Ficke, Cowger, Bergstrom, & Brodal, 2017). Fungicides belonging to the sterol
77 demethylation inhibitors group (DMIs) are commonly used in both agriculture and human
78 medicine (Price, Parker, Warrilow, Kelly, & Kelly, 2015). DMI-resistant strains of *P. nodorum*
79 harboring point mutations in the gene encoding the targeted protein (CYP51) have been
80 reported in China, Denmark, Sweden and Switzerland (Pereira, McDonald, & Brunner,
81 2017). While the severity of SNB is influenced by environmental factors (e.g. SNB is most
82 damaging in warm and moist conditions (Shaw, Bearchell, Fitt, & Fraaije, 2008; Zearfoss,
83 Cowger, & Ojiambo, 2011), the costs of managing SNB were estimated to be $108 m per
84 year in Australia alone (Murray & Brennan, 2009). A better understanding of the
85 evolutionary processes affecting local adaptation may provide insights into how to improve
86 management strategies and potentially predict future evolutionary changes in *P. nodorum*
87 populations.

88 Our aims in this study were to investigate the effects of natural selection and
89 genetic drift on quantitative traits using eight populations of *P. nodorum* sampled from
90 naturally infected farmer's fields around the world. First, we estimated the additive genetic
91 variation for colony growth and melanization phenotypes following exposure to a range of

92 different temperatures (providing a measure of thermal sensitivity) and fungicide
93 concentrations (providing a measure of fungicide sensitivity). We accomplished this by
94 measuring colony growth rates and melanization for 164 strains of *P. nodorum* using
95 automated image analysis (Lendenmann, Croll, Stewart, & McDonald, 2014; Lendenmann,
96 Croll, & McDonald, 2015). Next, we determined the degree of population genetic structure
97 among the eight populations using nearly 50,000 neutral SNPs extracted from whole-
98 genome sequences for all 164 strains. Finally, we estimated $Q_{ST}$ values for each trait and
99 compared these values to the $F_{ST}$ index calculated across the 8 populations. The $Q_{ST}$ - $F_{ST}$
100 comparisons allowed us to infer the predominant evolutionary forces driving quantitative
101 trait divergence among these populations and allowed us to detect local adaptation in
102 response to high temperatures and fungicide exposure.
103
104 **MATERIAL AND METHODS**
105 *Fungal populations and preparation of inoculum used for phenotyping*
106 *P. nodorum* strains were sampled between 1991 and 2005 from eight wheat fields
107 growing in eight different locations, including Australia, China, Iran, New York (USA),
108 Oregon (USA), South Africa, Switzerland and Texas (USA). Details regarding sampling sites
109 and population genetic structure based on SSR markers were described previously
110 (McDonald, Razavi, Friesen, Brunner, & McDonald, 2012; Stukenbrock et al., 2006). A total
111 of 164 genetically distinct isolates were analyzed with an average of ~21 isolates per
112 geographical field population (Table 1).
113 Based on preliminary experiments, we used 5 mm diameter plugs of mycelium as
114 initial inoculum for all experiments. All isolates were retrieved from -80°C long-term

115 storage on silica gel and transferred to Petri dishes containing Potato Dextrose Agar (PDA,
116 4 g $L^{-1}$ potato starch, 20 g $L^{-1}$ dextrose, 15 g $L^{-1}$ agar and 50 mg $L^{-1}$ kanamycin). The PDA
117 plates were grown for three days in the dark at a constant temperature of 24°C. 5 mm
118 diameter plugs of mycelium were cut from the edge of the growing colonies using a
119 sterilized cork borer and placed onto the center of fresh PDA Petri dishes. These plates
120 were grown in the dark at 24°C for seven days and then used as the inoculum source for all
121 experiments.
122
123 *Strain phenotyping*
124 All 164 isolates were exposed to the same seven environments, including low,
125 optimum and high growth temperatures and four different concentrations of an azole
126 fungicide. The experiments were conducted in square Petri dishes (120 x 120 x 17 mm,
127 Huberlab) containing PDA. Four 5 mm mycelium plugs of each strain were placed into the
128 corners of a square plate with equidistant separation. Each treatment was replicated twice,
129 generating eight colonies in total for each strain.
130 For the thermal response experiment, all isolates were grown in the dark on PDA at
131 18°C, 24°C and 30°C. Based on the outcomes of preliminary experiments using a subset of
132 16 of the strains (two from each field population), 18°C and 30°C were chosen to represent
133 stressful temperatures while 24°C was chosen as an optimum temperature for growth. For
134 the fungicide stress experiment, all isolates were grown at 24°C on PDA amended with
135 propiconazole (Syngenta, Basel, Switzerland) at either 0, 0.1, 0.5 or 1 ppm. All inoculation
136 procedures were performed on the same day for each of three separate batches of
137 approximately 54 isolates. No significant differences could be attributed to batch effects.

138 Digital images for each environment were taken at 2, 4, 6 and 8 days after
139 inoculation (DAI), a total of four time points. All camera settings and configurations, plate
140 orientations, and lighting conditions were standardized as described previously
141 (Lendenmann et al., 2014). After acquiring images, the plates were returned to their
142 growth chambers and their positions in the growth chamber were re-randomized. The
143 images were automatically analyzed using a modified version of a batch macro developed
144 for ImageJ (Lendenmann et al., 2014). For the new macro, the conversion from pixels to
145 square millimeters was performed using a calibration image taken from 50 cm above the
146 Petri dish. Colony detection was performed using the color threshold option, with the hue
147 sliding scales varying between 22 and 255 (macro lines 70 and 71) (Supplementary 1).
148 Quantitative measurements were acquired from image analyses for each colony.
149 Total colony area ($mm^2$) and mean grey value per colony (GV, a proxy for total melanization
150 on the 0-255 grey scale, where 0 is completely black and 255 is completely white) were
151 measured from digital images taken through the Petri dish top for colony size measures
152 and the Petri dish bottom for GV measures. We obtained a total of 8 raw data points per
153 isolate at each time point in each environment. The raw measures of total colony area and
154 GV were used to determine the following traits: (i) Radial growth rate was obtained by
155 fitting the mean colony radii ($\sqrt{total\ colony\ area/\pi}$) over the four time points using a
156 general linear model, resulting in average $r^2 > 0.9$ (Trinci 1971; Lendenmann et al. 2015).
157 Relative growth rates reflecting (ii) fungicide resistance and (iii) temperature sensitivity (TS)
158 were determined for each isolate as the ratio between growth rates under different
159 fungicide concentrations compared to the absence of fungicide, and growth rates at 18°C
160 or 30°C compared to 24°C. (iv) Melanization rate (MRate) was obtained by fitting the

161 distribution of GVs over the four time points using a general linear model. A positive value
162 for MRate indicates a decrease in melanization and a negative value for MRate indicates
163 an increase in colony melanization over time. The (v) melanization response (MResp) trait
164 was determined as the ratio between GV under a given fungicide dose and in the absence
165 of fungicide; and as the ratio between GV at 18°C or 30°C against 24°C. When MResp > 1 it
166 represents a decrease in melanization and MResp < 1 represents an increase in
167 melanization after stress exposure relative to optimum conditions. Variation among
168 isolates for GV reached its maximum at 8 DAI, so MResp was calculated based on this time
169 point.
170
171 *Strain genotyping*
172 Entire genome sequences were generated for all 164 strains. Strains were grown in
173 Potato Dextrose Broth (PDB) and total DNA was extracted from lyophilized mycelium using
174 DNeasy Plant Mini Kits (Qiagen) according to the manufacturer's instructions. Whole-
175 genome sequencing was performed on an Illumina HiSeq 2500 platform, with paired-end
176 reads of 150 bp. All the Illumina sequence data are available in the NCBI Short Read Archive
177 (accession xxx).
178 The generated raw reads were trimmed for remaining Illumina adapters and read
179 quality with Trimmomatic v0.36 (Bolger, Lohse, & Usadel, 2014), using the following
180 settings: illuminaclip = TruSeq3-PE.fa:2:30:10, leading = 10, trailing = 10, slidingwindow =
181 5:10, minlen = 50. Trimmed reads were aligned with the reference isolate SN2000
182 (Richards, Wyatt, Liu, Faris, & Friesen, 2017), which is assembled into chromosomes. The
183 alignment was performed with the short-read aligner Bowtie 2 version 2.3.3 (Langmead &

184 Salzberg, 2012), using the --very-sensitive-local option. Duplicated PCR reads were marked
185 as duplicate using Picard tools version 2.17.2 (http://broadinstitute.github.io/picard).
186 Single nucleotide polymorphism (SNP) calling and variant filtration were performed
187 using the Genome Analysis Toolkit (GATK) version 3.8-0 (McKenna et al., 2010). First, we
188 used HaplotypeCaller in each isolate file individually, with the -emitRefConfidence GVCF
189 and -ploidy 1 options. Then, joint variant calls were performed using GenotypeGVCFs with
190 the flag -maxAltAlleles 2. Finally, SelectVariants and VariantFiltration was used for hard
191 filtering SNPs with the following cut-offs: QUAL < 200; QD < 10.0; MQ < 20.0; –2 >
192 BaseQRankSum > 2; – 2 > MQRankSum > 2; –2 > ReadPosRankSum > 2; FS > 0.1.
193 We retained only bi-allelic sites and excluded sites with missing data using vcftools
194 0.1.15 (Danecek et al., 2011). Using the function --indep-pairwise in plink v1.9 we pruned
195 SNPs above a linkage disequilibrium threshold of 0.2 using a sliding window of 15 kb (Chang
196 et al., 2015). From this unlinked SNP dataset, we selected only SNPs causing synonymous
197 substitutions (on four-fold degenerated sites) to identify neutral SNP markers, using the
198 software VCF2MK (https://github.com/russcd/vcf2MK). The final data set consisted of
199 49374 neutral and un-linked SNPs.
200
201 *Data Analyses*
202 We applied a general linear model to determine whether there were significant
203 effects for populations and isolates nested within populations on the trait values (package
204 "lm" and function anova in R) (R Core Team, 2019). Among population comparisons of
205 mean growth rate and mean melanization in the different environments were based on
206 Tukey's honest significance difference test using R.

207 Within-population components of variance for each trait were determined using
208 genetic variance and heritability (Willi et al., 2011; Stefansson et al., 2014; Pereira et al.,
209 2016). The variance components were determined using a statistical procedure
210 implemented in R software using the lme4 package (Bates, Mächler, Bolker, & Walker,
211 2015). The variance derived from the isolates within each population was interpreted as
212 genetic variance ($V_G$), while variance among replicates of the same clone was interpreted
213 as environmental variance because replicates had the same genotype. Narrow-sense
214 heritability ($h^2$) was calculated as the ratio between $V_G$ and total phenotypic variation
215 within a population (Falconer & Mackay, 1996). Confidence intervals were estimated by
216 applying a bootstrap with 999 re-samples.

217 Estimates of population divergence ($F_{ST}$) were calculated using the 49374 retained
218 SNPs with the R package hierfstat (Goudet, 2005). Overall and among population values of
219 $F_{ST}$ as well as their confidence intervals were determined by bootstrapping with 999
220 resamplings using hierfstat (Goudet, 2005). Nei's diversity was calculated using the
221 popgenome R package (Pfeifer, Wittelsbürger, Ramos-Onsins, & Lercher, 2014).

222 *P. nodorum* is a haploid organism, so dominance effects among alleles within loci
223 can be ignored. If we assume a small or negligible epistatic effect within populations,
224 genetic variance is equivalent to additive genetic variance for the determination of
225 population divergence in quantitative traits ($Q_{ST}$) (Whitlock, 2008). Under this scenario, the
226 following formula can be used to calculate $Q_{ST}$ as described by (Zhan et al., 2005):

227 $$Q_{ST} = \frac{\delta^2{}_{AP}}{\delta^2{}_{AP} + \delta^2{}_{WP}}$$

228 Where $\delta^2{}_{AP}$ is the additive genetic variance attributed to among-population variation and
229 $\delta^2{}_{WP}$ is the additive genetic variance attributed to within-population variation.

230 Correlation analyses among the 12 traits used in the $Q_{ST}/F_{ST}$ analysis, between
231 overall heritability and Nei's diversity, between MRate and fungicide resistance/growth
232 rate and between MResp and growth rate and MRate were performed using a general
233 linear model based on Pearson's coefficient in the R package RcmdrMisc (Fox, 2005), and
234 visually represented using the R package ggplot2 (Wickham, 2009).

235 The thermal reaction norm of *P. nodorum* was modelled based on a second-order
236 polynomial equation using individual measures of average growth rate for every isolate
237 across the three tested temperatures. Another measure, the composite reaction norm, was
238 calculated based on the slope of the reaction norm between 24°C and 18°C and between
239 24°C and 30°C. An average value was calculated from the two slopes and populations were
240 compared based on these isolate mean values.

241

242 **RESULTS**

243 *Colony growth rate and melanization show quantitative distributions and high heritabilities*

244 Phenotypic variation for traits related to growth and melanization in *P. nodorum*
245 was assessed after exposure to different temperatures and different concentrations of an
246 azole fungicide for eight geographical field populations (Figure 1). As expected, the
247 environment of 24°C without fungicide, hereafter referred to as the control environment,
248 provided the fastest growth rate for most isolates. We found near-normal distributions for
249 growth rate and melanization in the control environment and at 18°C and 30°C, consistent
250 with quantitative inheritance of these traits (Figure 1). Growth rates at 0.1, 0.5 and 1 ppm
251 fungicide showed bimodal distributions (Figure 1). In general, all environments significantly

252 affected the average trait values across all populations and across all isolates within
253 populations ($P \leq 0.0001$, Table 2).

254 We observed high heritability ($h^2$) values for growth rate and melanization in the
255 different environments (Table 3). $h^2$ ranged from a low of 0.58 for melanization in 0.5 ppm
256 propiconazole to a high of 0.95 for growth rate in the control environment and at 18°C and
257 30°C. Other traits with $h^2$ higher than 0.9 were growth rates in 0.1 ppm, 0.5 ppm, and 1
258 ppm propiconazole and melanization in the control environment, 18°C, 30°C and in 0.1 ppm
259 propiconazole.

260

261 *Extreme temperatures and fungicide exposure reduced growth rates*

262 In the optimal control environment, the Australian population had a significantly
263 lower growth rate (4.37 mm/day) than all other populations except South Africa ($P \leq 0.05$,
264 Table 4). Average growth rates slowed as propiconazole concentrations increased ($P \leq$
265 $0.001$). At 0.1 ppm, the Chinese and Swiss populations had the fastest growth rates (4.6
266 and 4.3 mm/day, respectively; $P \leq 0.05$; Table 4), while the populations from Australia,
267 Oregon and South Africa had the slowest growth rates (2.6, 2.4 and 2.5 mm/day,
268 respectively; $P \leq 0.05$; Table 4). At the highest propiconazole concentrations (0.5 and 1
269 ppm), the Chinese population grew the fastest (3.3 and 2.4 mm/day, respectively; $P \leq 0.05$;
270 Table 4), followed by Switzerland (2.7 and 1.9 mm/day, respectively; $P \leq 0.05$; Table 4), with
271 both populations showing significantly lower fungicide sensitivity than the other
272 populations. No differences were detected among the other populations at these two
273 concentrations.

274 Temperatures of 18°C and 30°C significantly reduced the average growth rates
275 compared to the control temperature ($P \leq 0.001$). At 18°C, the fastest growth rate was in
276 the New York population, and the slowest was in Australia (4.4 and 3.6 mm/day,
277 respectively, $P \leq 0.05$, Table 4). At 30°C, there were no significant differences among
278 populations except for South Africa, which had the slowest growth rate (1.9 mm/day, $P \leq$
279 0.05, Table 4). Based on the TS calculations, the populations were overall more sensitive to
280 higher temperatures then to lower temperatures (Supplementary 2). For TS at the higher
281 temperature, the populations from Australia and Texas were the least sensitive (TS values
282 were closest to 1), whereas the population from South Africa was the most sensitive. For
283 TS at the lower temperature, the populations from New York and Australia were the least
284 affected. Altogether, 15 isolates had TS > 1 at the lower temperature and no isolate had TS
285 > 1 at the higher temperature.
286 The thermal reaction norm of *P. nodorum*, which reflects the patterns of growth
287 rate across the tested temperatures, showed a good fit to a second-order polynomial
288 model (Supplementary 3). On average, this model accounted for 66% of the total variation
289 for growth rates in *P. nodorum* ($P \leq 0.001$). We did not find significant differences among
290 populations using this composite reaction norm.
291
292 *Melanization varied according to environmental conditions*
293 In the control environment, the strains in the population from Oregon showed
294 significantly lower melanization (i.e. higher GVs) than the populations from Australia,
295 China, Switzerland and Texas ($P \leq 0.05$; Table 4). On average, more stressful temperatures
296 and fungicide stress significantly affected melanization ($P \leq 0.001$).

297 Melanization was significantly higher at 0.5 ppm then at 0 and 0.1 ppm of
298 propiconazole across all populations ($P \leq 0.001$), with mean GVs of 66, 82 and 77
299 respectively (Table 4). Average melanization across populations at 1 ppm (GV = 68) was not
300 significantly different from melanization at 0.5 ppm (Table 4). Texas was the most
301 melanized population at 0.1 ppm, while Australia was the most melanized population at
302 0.5 and 1 ppm propiconazole ($P \leq 0.05$, Table 4).
303 Across all populations we observed higher melanization at 30°C and lower
304 melanization at 18°C (mean GVs of 61 and 90 respectively, $P \leq 0.001$, Table 4). At the
305 highest temperature, Texas was the most melanized population and at the lowest
306 temperature Australia showed the highest amount of melanization (mean GVs of 47 and
307 81 respectively).
308
309 *Low population structure based on neutral genome-wide SNPs*
310 We calculated the genome-wide $F_{ST}$ using 49374 unlinked SNPs (Supplementary 4).
311 The overall $F_{ST}$ across populations was 0.12 ($P \leq 0.0001$). The pairwise $F_{ST}$ ranged from 0.24
312 between Australia and Iran to no differentiation between China and Switzerland (Table 5).
313 Iran was the population with the highest overall Nei's diversity (Table 4, $P \leq 0.05$, 0.13),
314 consistent with previous studies placing the *P. nodorum* center of origin in the fertile
315 crescent (McDonald et al., 2012).
316
317 *Natural selection was the predominant evolutionary force acting on P. nodorum*
318 *populations*

319 To disentangle the effects of natural selection and genetic drift on quantitative
320 traits in populations of *P. nodorum*, we compared the $Q_{ST}$ index for each trait to the $F_{ST}$
321 index (Figure 2). The $Q_{ST}$ values for melanization were consistently lower than $F_{ST}$ across all
322 environments (Figure 2, $P \leq 0.0001$), suggesting that melanization is under stabilizing
323 selection. Growth rates in all environments, except for the control environment and 18°C,
324 had significantly higher $Q_{ST}$ then $F_{ST}$ (Figure 2, $P \leq 0.0001$), suggesting that selection
325 operates to favor local adaptation for these traits.
326
327 *Trait correlations*
328 The correlation analysis revealed significant positive correlations among growth
329 rates and among GVs (Figure 3, $P \leq 0.0001$), but no significant correlations were found
330 between growth rates and GVs for any treatment. Overall growth rates amongst the three
331 concentrations of fungicide were all significantly correlated, indicating that less sensitive
332 isolates maintained higher growth rates across all concentrations of propiconazole. Growth
333 rate in the control environment was correlated with growth rate at 18°C but not with
334 growth rate at 30°C. For melanization, we found positive correlations for GV at 0.1 ppm,
335 0.5 ppm, 1 ppm, 30°C, 18°C and the control environment. For instance, GV at 30°C was
336 moderately correlated with GVs at 0.1 and 0.5 ppm propiconazole ($R$ = 0.40 and 0.35
337 respectively, $P \leq 0.0001$) suggesting that melanin accumulates similarly under these
338 conditions.
339 Fungicide resistance and growth rates at different temperatures were significantly
340 correlated with melanization rates (Figure 4). We found significant correlations between
341 fungicide resistance and MRate at 0.5 and 1 ppm ($p \leq 0.001$, Figure 4A). At the higher

342 concentrations, isolates with more negative MRate displayed an overall increase in levels
343 of fungicide resistance. At 30°C, growth rate and MRate were significantly correlated
344 (Figure 4B), suggesting that isolates with higher MRate were growing faster. Analogous
345 patterns were observed for fungicide resistance and MResp (Supplementary 5A).
346 No significant correlations were found between TS and mean annual temperature
347 or annual temperature variation (Supplementary 2).
348
349 **DISCUSSION**
350 We combined a digital image phenotyping method with whole-genome sequencing
351 of 164 isolates from eight global field populations of the wheat pathogen *P. nodorum* to
352 infer the patterns of selection operating on different quantitative traits. When exposed to
353 a variety of temperatures and fungicide concentrations, we found differences in the
354 average growth rates, the degree of melanization, and trait heritability among populations.
355 We then differentiated among the evolutionary forces acting on traits related to thermal
356 and fungicide sensitivity.
357 Growth rates varied significantly among populations, with the highest overall
358 growth rates at 24°C followed by 18°C. The least favorable temperature was 30°C. The field
359 populations from Australia and South Africa had the slowest growth rates at all
360 temperatures, while the populations from Australia and Texas were the least affected by
361 30°C according to the measures of TS. Temperature has an especially large impact on the
362 physiology of ectothermic organisms like fungi because their internal temperature directly
363 reflects the external thermal environment (Angilletta, Oufiero, & Leaché, 2006; Knies &
364 Kingsolver, 2010). In general, phenotypic plasticity and genetic differentiation are

365 considered the main mechanisms underlying the evolution of thermal adaptation (Chevin,
366 Lande, & Mace, 2010; Cooper, Tharp, Jernberg, & Angilletta, 2012; Tonsor, Elnaccash, &
367 Scheiner, 2013; Yampolsky, Schaer, & Ebert, 2013). On average, we found that plasticity
368 made only a small contribution (<5%) to overall phenotype variation. The field populations
369 from Australia and South Africa had both the slowest overall growth rates and the lowest
370 levels of genetic diversity. We hypothesize that the slow growth rates in these populations
371 reflects a lower evolutionary potential due to a founder effect (Carson 1961; Templeton et
372 al. 2001), as also seen for Australian populations of *Z. tritici* and *R. commune* (Zhan &
373 McDonald, 2011; Stefansson et al., 2014). The Australian and South African populations of
374 *P. nodorum* likely originated on infected seeds when Europeans introduced wheat into
375 these regions during the last 500 years, providing a restricted gene pool (Stukenbrock et
376 al., 2006). Subsequent gene flow that could increase local genetic diversity during the
377 modern era may have been prevented by global trading patterns (Australia is a major
378 wheat exporter and South Africa imports relatively little wheat) coupled with effective
379 quarantine measures that limited the introduction of additional infected wheat seeds or
380 grains (Oliver et al., 2012).

381 The $Q_{ST}$ - $F_{ST}$ analyses indicated that growth at 18°C and 24°C were under stabilizing
382 selection ($Q_{ST} < F_{ST}$), while diversifying selection ($Q_{ST} > F_{ST}$) was the predominant
383 evolutionary force affecting growth at 30°C. We chose these three temperatures to
384 represent the range of temperatures that are likely to be encountered by many *P. nodorum*
385 populations during the wheat cropping season. It was postulated that field environments
386 experiencing a wide fluctuation in temperatures would favor isolates that can grow more
387 quickly and consequently colonize the host faster when conditions become conducive for

388 disease development (Stefansson, McDonald, & Willi, 2013; Yang et al., 2016). However,
389 because the pathogen depends on the host for reproduction, the pathogen's overall fitness
390 may be negatively affected if the host life span is reduced due to excessive host damage
391 caused by pathogen growth that is too rapid (Boots, Hudson, & Sasaki, 2004). This trade-
392 off between pathogen virulence and pathogen reproduction may stabilize rates of host
393 colonization in environments where optimum temperatures for infection and colonization
394 are more constant and frequent, offsetting the selective pressure that favors faster
395 growers (Alizon, Hurford, Mideo, & Baalen, 2009). The temperatures of 18°C and 24°C used
396 in our experiment appear closest to the optimum temperatures for *P. nodorum* growth and
397 development, consistent with the finding of stabilizing selection, which favors isolates with
398 growth rates closer to the population mean. The significantly higher population
399 differentiation at 30°C is consistent with a process of diversifying selection for local
400 adaptation. Over time, this selective process would be expected to evolve *P. nodorum*
401 populations that are locally adapted to higher temperatures (Hayden, Bratulic, Koenig,
402 Ferrada, & Wagner, 2014; Yang et al., 2016). Given current patterns of global trade, strains
403 of *P. nodorum* that are adapted to higher temperatures in wheat exporting countries like
404 Australia could be unintentionally introduced into regions such as China where local
405 populations are maladapted to high temperatures. The long distance movement of new
406 strains of the wheat yellow rust fungus showing novel temperature adaptations caused
407 extensive damage (Hovmoller, Yahyaoui, Milus, & Justesen, 2008). Thus *P. nodorum* joins
408 the ranks of plant pathogens that are likely to pose an increasing risk to global food security
409 in a warming world (Hovmoller et al., 2008; Milus, Kristensen, & Hovmøller, 2009; Fisher et
410 al., 2012; Stefansson et al., 2013).

411 Directional selection ($Q_{ST}$ > $F_{ST}$) was associated with growth rates at all tested
412 fungicide concentrations, indicating that natural selection is the main contributor to
413 population differentiation for fungicide sensitivity. We extracted and analyzed the *CYP51*
414 gene from the genome sequences of all 164 isolates used in this $Q_{ST}$ - $F_{ST}$ analysis, and
415 confirmed the occurrence of previously reported *CYP51* mutations in isolates exhibiting the
416 highest fungicide resistance (Pereira et al., 2017). The observed mutations, found only in
417 the populations from China and Switzerland, are likely responsible for most of the
418 differences in growth rate at different fungicide concentrations among populations.

419 Evidence that directional selection shapes local adaptation for fungicide resistance
420 was also found in the wheat pathogen *Zymoseptoria tritici* (Zhan et al., 2005), while in
421 *Rhynchosporium commune* and *Phytophthora infestans* it was found to be under stabilizing
422 selection (Stefansson et al., 2014; Qin et al., 2016). In *Z. tritici* the emergence of *CYP51*
423 mutations in the pathogen populations was proposed to occur locally and then spread via
424 gene flow across Europe or, as shown more recently, across Tasmania (Brunner, Stefanato,
425 & McDonald, 2008; McDonald et al., 2018). *P. nodorum* and *Z. tritici* frequently coinfect
426 wheat plants in the field (Gilbert & Woods, 2001; Blixt, Olson, Lindahl, Djurle, & Yuen, 2010;
427 Oliver et al., 2012). Though the majority of fungicides applied to wheat in Europe target *Z.*
428 *tritici* (Fones & Gurr, 2015), we hypothesize that these treatments indirectly selected for
429 fungicide resistance in populations of *P. nodorum* (Knorr, Jørgensen, & Nicolaisen, 2019).
430 The findings of CYP51 mutations associated with azole resistance, high heritability, and
431 evidence for diversifying selection favoring local adaptation suggest a significant risk for
432 emergence and spread of azole resistance over larger geographical scales for *P. nodorum*.

433 Melanin is a secondary metabolite found broadly across eukaryotes that often
434 displays complex phenotypic variation across an organism's life cycle (Butler & Day, 1998;
435 Chumley & Valent, 1990; Dadachova & Casadevall, 2008; Singaravelan et al., 2008; Sturm
436 & Duffy, 2012). The ecological roles associated with fungal melanin vary widely among
437 species (Butler & Day, 1998), but it is most often reported to be related to virulence,
438 competition with other microbes, protection against UV-light and toxic compounds, and
439 tolerance of extreme temperatures (Nosanchuk & Casadevall, 2003; Dadachova et al.,
440 2007; Hagiwara et al., 2017). Although melanin is thought to provide protection against
441 cold and heat stress (Rehnstrom & Free, 1996; Paolo et al., 2006), there are exceptions
442 (Wheeler & Bell, 1988), and information regarding its impact on fungal thermal tolerance
443 remains scarce (Cordero & Casadevall, 2017). Melanin production is energetically costly
444 (Calvo, Wilson, Bok, & Keller, 2002), and may impose a fitness penalty if it reduces growth
445 (Choi & Goodwin, 2011; Krishnan et al., 2018).
446 Quantitative measures of melanization in fungal colonies were previously used to
447 infer possible contributions of melanin to variation in temperature and fungicide sensitivity
448 in the fungi *Z. tritici* and *R. commune* (Lendenmann et al., 2014; T. Stefansson et al., 2014;
449 Lendenmann et al., 2015; Zhu, Zhan, & McDonald, 2018). In *P. nodorum* we found that
450 stabilizing selection was the predominant evolutionary force shaping differences in
451 melanization across all tested conditions. The low differentiation among populations for
452 melanization suggests that selection operates against extreme phenotypes in *P. nodorum*
453 (Sanjak, Sidorenko, Robinson, Thornton, & Visscher, 2018). For the barley scald pathogen
454 *R. commune*, melanization was also found to be under stabilizing selection (Stefansson et
455 al., 2014). In *R. commune*, higher melanization was positively correlated with higher growth

456 rates at 18°C and 22°C, as well as increased fungicide resistance (Zhu et al., 2018).
457 Melanization was also correlated with faster growth rates at 15°C and reduced fungicide
458 sensitivity in *Z. tritici* (Lendenmann et al., 2014, 2015).

459 In *P. nodorum* the GV for most isolates was lowest at 30°C, suggesting that melanin
460 production increases under heat stress. We observed a negative correlation between
461 MRate and growth rate at 30°C ($P$ = 0.02), with faster growing colonies accumulating
462 melanin at a slower rate, but there was no correlation between growth rate and MRate at
463 18 or 24°C. Altogether, these findings suggest a possible trade-off between melanization
464 and growth rate under heat stress. The calculated values for both MRate and MResp
465 suggest that the strains that were slowest to melanize had the greatest resistance to
466 propiconazole, indicating that melanin production did not reduce azole sensitivity. In a
467 knockout study in *Z. tritici*, albino mutants lacking the melanin-related transcription factor
468 *Zmr1* were exposed to two different fungicides, and had their growth compared to the wild
469 type strain producing melanin (Krishnan et al., 2018). The fungicide bixafen (a succinate
470 dehydrogenase inhibitor, SDHI) significantly reduced the growth of the albino mutants
471 compared to the isogenic wild type strain, but there was no difference in the growth of the
472 strains exposed to propiconazole (Krishnan et al., 2018). The protective effect of melanin
473 against fungicides is attributed to its binding capacity which reduces the fungicide
474 availability (Bridelli, Ciati, & Crippa, 2006; Paolo et al., 2006; Eisenman & Casadevall, 2012).
475 Since melanin has a low binding affinity with azoles, the inefficient binding process may
476 limit its overall contribution to azole resistance (Nosanchuk & Casadevall, 2006), consistent
477 with our findings in *P. nodorum*.

Our findings illustrate how local environmental conditions can couple with different agricultural practices to shape the evolutionary trajectories of geographically distinct populations of a plant pathogen. The high heritability for traits related to fungicide and thermal sensitivity indicate the importance of genetic diversity in affecting the adaptative potential of *P. nodorum*. We found that directional selection favors genotypes with faster growth rates under fungicide and high temperature stress. This suggests a significant risk for *P. nodorum* to develop fungicide resistance. Moreover, under the expected scenario of global warming, it is likely that SNB will easily adapt to susceptible wheat crops growing in warmer areas.

**Acknowledgements**

We thank Daniel Croll for his assistance and suggestions on the analyses of raw genome sequences. This study was financed in part by the "Coordenação de Aperfeiçoamento de Pessoal de Nível Superior - Brasil (CAPES)" - Finance Code 001. Marcello Zala provided technical assistance. The Genetic Diversity Center (GDC) – ETH Zurich and the Functional Genomics Center in Zurich provided sequencing facilities.

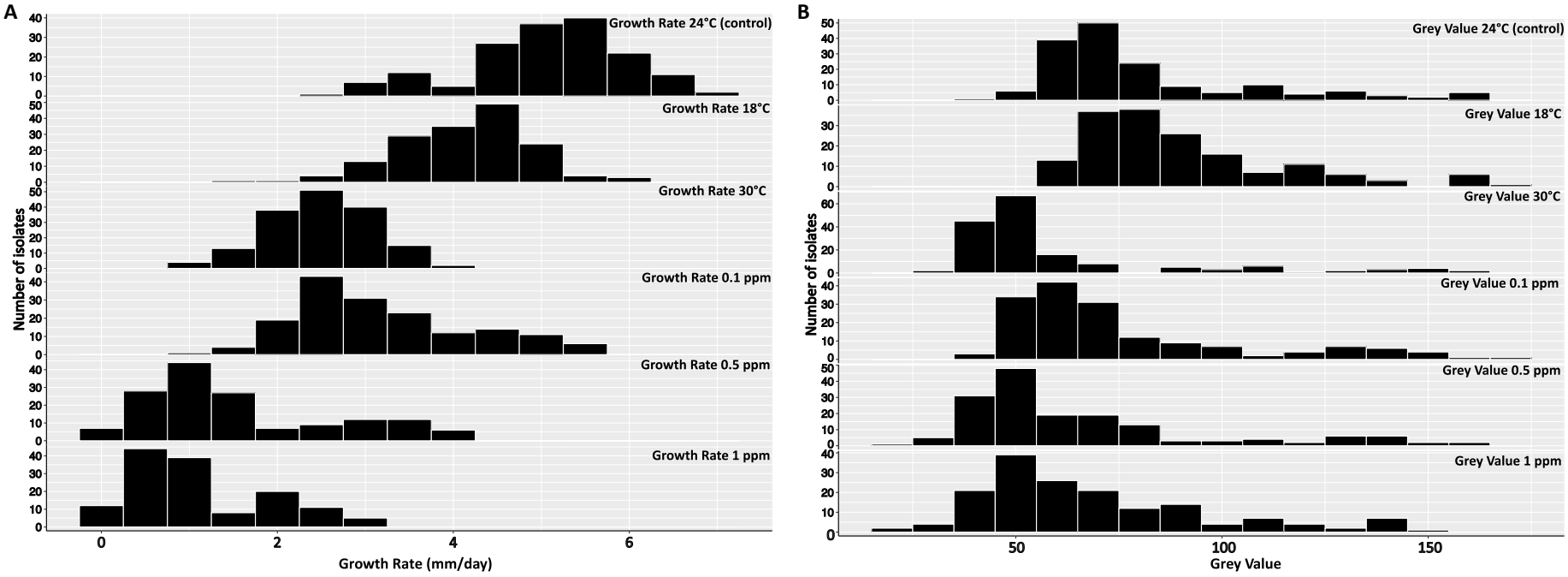


FIGURE 1 The distribution of growth rate (A) and grey value (B) for 164 isolates of *Parastagonospora nodorum* growing under different temperatures and fungicide concentrations. Each plot within a panel represents a different temperature or fungicide treatment as indicated in the aligned text.

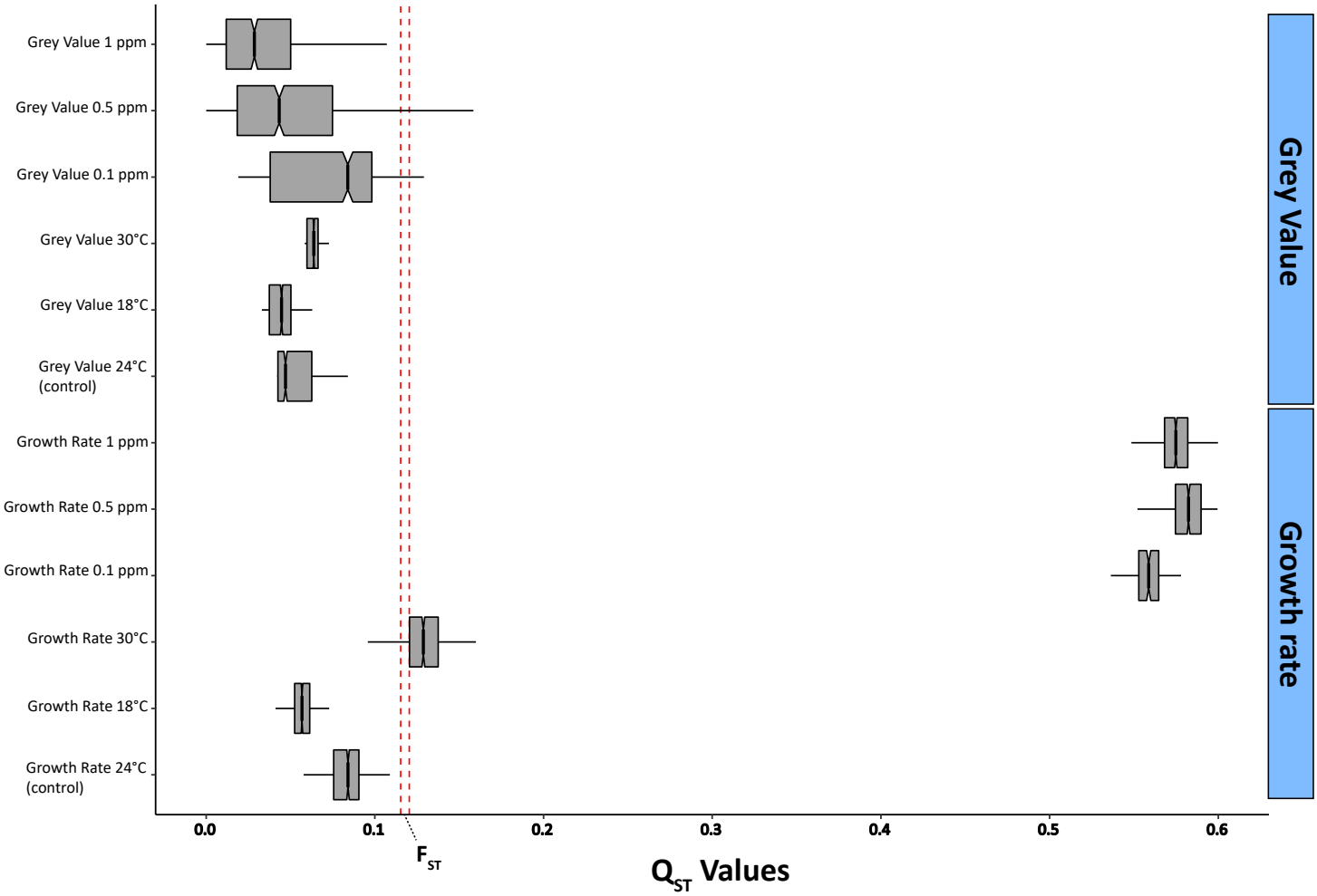


FIGURE 2 Comparisons of $Q_{ST}$ - $F_{ST}$ across 12 quantitative traits of *Parastagonospora nodorum*. Boxplots display the confidence intervals determined by bootstrapping with 999 resamplings of $Q_{ST}$ values. The red dashed lines show the overall $F_{ST}$ distribution. Traits with a $Q_{ST}$ distribution below that range are interpreted as being under stabilizing selection, while traits with $Q_{ST}$ distribution above that range are interpreted as being under diversifying selection.

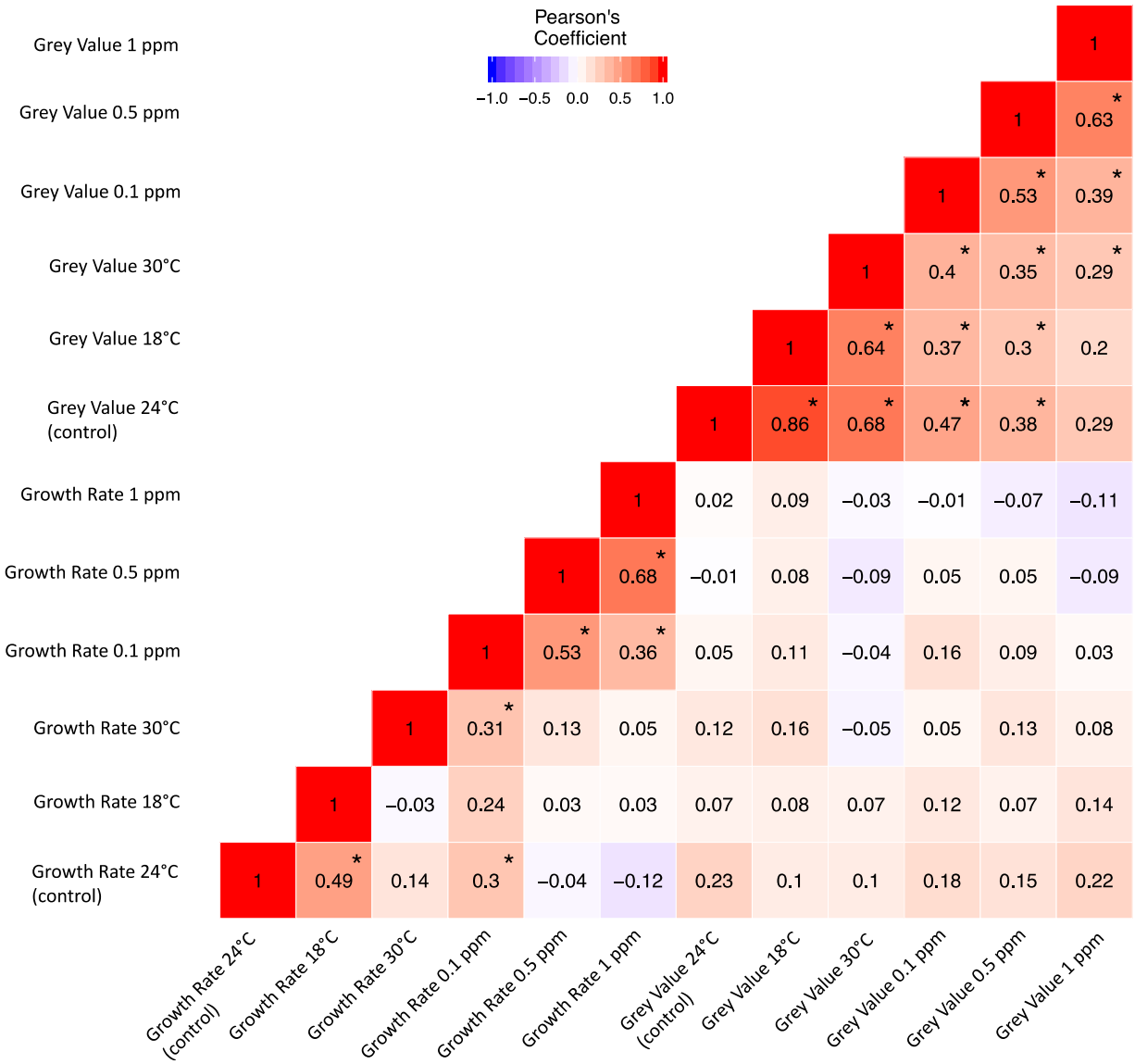


FIGURE 3 Pairwise correlations among 12 quantitative traits of *Parastagonospora nodorum*. To make data comparable across populations, trait values of each trait-population combination were standardized to a mean of 0 and a standard deviation of 1, and then correlation analyses were performed based on isolate means. Significance levels were determined after Bonferroni correction for multiple comparisons. * Significant at $p < 0.0001$).

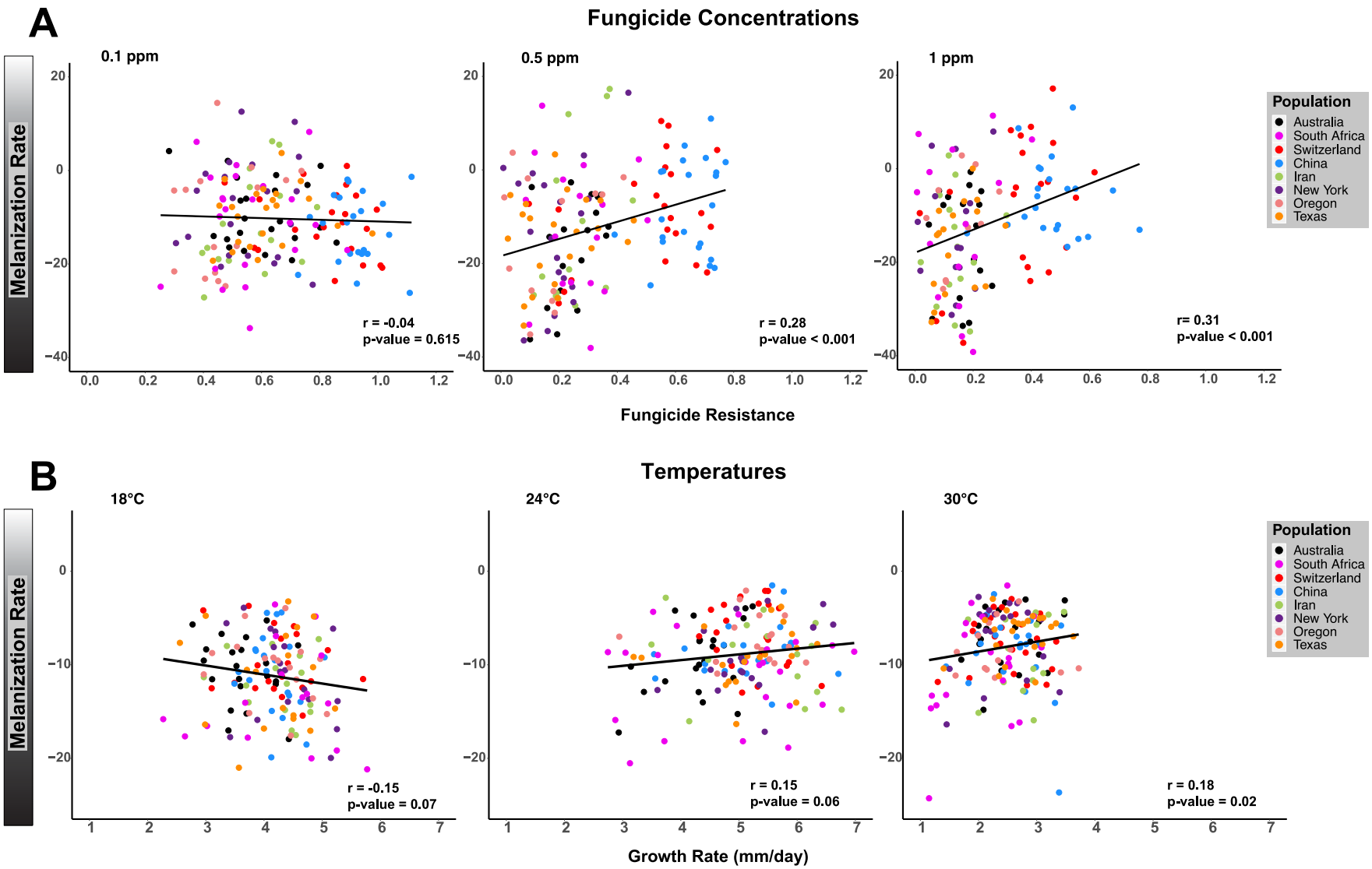


FIGURE 4 Correlation analysis between melanization rate (calculated from the slope of a line fitted to GV over time) and (A) fungicide resistance (= growth rate in presence of fungicide / growth rate in absence of fungicide) and (B) growth rate of isolates under different temperatures. The dots represent individual isolates and colors the corresponding population of origin.

TABLE 1 Origin, location, year of collection and sample size (*N*) of *Parastagonospora nodorum* populations included in the $Q_{ST}$-$F_{ST}$ analysis.

| Origin | Location | Year | *N* | Collector(s) |
|---|---|---|---|---|
| *Oceania* | | | | |
| Australia | Narrogin | 2001 | 22 | B.A. McDonald & R. Loughman |
| *Africa* | | | | |
| South Africa | Southwestern Cape | 1995 | 22 | P. Crous |
| *Europe* | | | | |
| Switzerland | Winterthur | 1999 | 22 | B.A. McDonald & V. Michel |
| *Asia* | | | | |
| China | Fujian Province | 2001 | 22 | R. Wu |
| Iran | Golestan Province | 2005/2010 | 16 | R. Sommerhalder & M. Razavi |
| *North America* | | | | |
| New York | Ithaca | 1991 | 21 | G. Bergstrom |
| Oregon | Hyslop | 1993 | 17 | M. Schmidt |
| Texas | Overton | 1992 | 22 | B.A. McDonald & L. Nelson |
| Totals | | 1992-2010 | 164 | |

TABLE 2 General linear model analyses testing the effect of population and isolate (nested within population) on quantitative traits of *Parastagonospora nodorum*.

| Trait | Source | df | MS | F | *P* |
|---|---|---|---|---|---|
| Growth Rate 24°C (control) | Population | 7 | 4.22 | 77.08 | <0.0001 |
| | Isolates within population | 156 | 1.45 | 26.52 | <0.0001 |
| | Error | 164 | 0.05 | NA | NA |
| Growth Rate 18°C | Population | 7 | 2.41 | 54.10 | <0.0001 |
| | Isolates within population | 156 | 1.17 | 26.27 | <0.0001 |
| | Error | 164 | 0.04 | NA | NA |
| Growth Rate 30°C | Population | 7 | 2.40 | 76.40 | <0.0001 |
| | Isolates within population | 156 | 0.70 | 22.32 | <0.0001 |
| | Error | 164 | 0.03 | NA | NA |
| Growth Rate 0.1 ppm | Population | 7 | 31.16 | 620.08 | <0.0001 |
| | Isolates within population | 156 | 0.71 | 14.04 | <0.0001 |
| | Error | 164 | 0.05 | NA | NA |
| Growth Rate 0.5 ppm | Population | 7 | 40.11 | 640.44 | <0.0001 |
| | Isolates within population | 156 | 0.82 | 13.03 | <0.0001 |
| | Error | 164 | 0.06 | NA | NA |
| Growth Rate 1 ppm | Population | 7 | 23.66 | 579.90 | <0.0001 |
| | Isolates within population | 156 | 0.53 | 12.88 | <0.0001 |
| | Error | 164 | 0.04 | NA | NA |
| Grey Value 24°C (control) | Population | 7 | 6712.08 | 52.06 | <0.0001 |
| | Isolates within population | 156 | 1553.06 | 12.05 | <0.0001 |
| | Error | 164 | 128.92 | NA | NA |
| Grey Value 18°C | Population | 7 | 3048.37 | 39.32 | <0.0001 |
| | Isolates within population | 156 | 1068.70 | 13.78 | <0.0001 |
| | Error | 164 | 77.53 | NA | NA |
| Grey Value 30°C | Population | 7 | 5365.80 | 345.83 | <0.0001 |
| | Isolates within population | 156 | 1465.98 | 94.48 | <0.0001 |
| | Error | 164 | 15.52 | NA | NA |
| Grey Value 0.1 ppm | Population | 7 | 5190.23 | 84.33 | <0.0001 |
| | Isolates within population | 156 | 1693.65 | 27.52 | <0.0001 |
| | Error | 164 | 61.55 | NA | NA |
| Grey Value 0.5 ppm | Population | 7 | 4181.42 | 9.85 | <0.0001 |
| | Isolates within population | 156 | 1710.79 | 4.03 | <0.0001 |
| | Error | 164 | 424.37 | NA | NA |
| Grey Value 1 ppm | Population | 7 | 4008.38 | 10.36 | <0.0001 |
| | Isolates within population | 156 | 1402.31 | 3.62 | <0.0001 |
| | Error | 164 | 386.93 | NA | NA |

TABLE 3 Heritability measures, standard deviations (SD) and coefficient of variation (CV) for 12 quantitative traits of *Parastagonospora nodorum*.

| **Population** | Growth Rate 24°C (control) | Growth Rate 18°C | Growth Rate 30°C | Growth Rate 0.1 ppm | Growth Rate 0.5 ppm | Growth Rate 1 ppm | Grey Value 24°C (control) | Grey Value 18°C | Grey Value 30°C | Grey Value 0.1 ppm | Grey Value 0.5 ppm | Grey Value 1 ppm |
|---|---|---|---|---|---|---|---|---|---|---|---|---|
| **Australia** | 0.96 | 0.92 | 0.99 | 0.98 | 0.82 | 0.79 | 0.96 | 0.97 | 0.98 | 0.97 | 0.39 | 0.49 |
| | 0.02 | 0.05 | 0.01 | 0.01 | 0.09 | 0.11 | 0.02 | 0.02 | 0.01 | 0.02 | 0.32 | 0.45 |
| **South Africa** | 0.99 | 0.91 | 0.96 | 0.63 | 0.89 | 0.92 | 0.98 | 0.51 | 0.59 | 0.60 | 0.44 | 0.97 |
| | 0.01 | 0.08 | 0.03 | 0.31 | 0.07 | 0.04 | 0.01 | 0.49 | 0.39 | 0.37 | 0.34 | 0.02 |
| **Switzerland** | 0.93 | 0.98 | 0.79 | 0.97 | 0.98 | 0.97 | 0.98 | 0.98 | 0.98 | 0.99 | 0.92 | 0.69 |
| | 0.03 | 0.01 | 0.21 | 0.02 | 0.01 | 0.02 | 0.01 | 0.01 | 0.00 | 0.01 | 0.07 | 0.31 |
| **China** | 0.97 | 0.95 | 0.99 | 0.94 | 0.98 | 0.96 | 0.99 | 0.99 | 0.98 | 0.96 | 0.98 | 0.99 |
| | 0.01 | 0.02 | 0.00 | 0.03 | 0.01 | 0.02 | 0.00 | 0.00 | 0.01 | 0.02 | 0.01 | 0.01 |
| **Iran** | 0.99 | 0.92 | 0.99 | 0.95 | 0.93 | 0.92 | 0.98 | 0.99 | 0.97 | 0.98 | 0.50 | 0.48 |
| | 0.00 | 0.06 | 0.00 | 0.02 | 0.05 | 0.04 | 0.00 | 0.01 | 0.00 | 0.01 | 0.33 | 0.39 |
| **New York** | 0.98 | 0.98 | 0.96 | 0.99 | 0.77 | 0.86 | 0.66 | 0.99 | 0.98 | 0.97 | 0.52 | 0.66 |
| | 0.01 | 0.01 | 0.04 | 0.00 | 0.19 | 0.08 | 0.35 | 0.00 | 0.00 | 0.01 | 0.44 | 0.32 |
| **Oregon** | 0.77 | 0.93 | 0.98 | 0.92 | 0.98 | 0.94 | 0.98 | 0.99 | 0.98 | 0.98 | 0.47 | 0.34 |
| | 0.18 | 0.06 | 0.01 | 0.06 | 0.01 | 0.02 | 0.00 | 0.00 | 0.00 | 0.01 | 0.39 | 0.34 |
| **Texas** | 0.98 | 0.98 | 0.97 | 0.97 | 0.93 | 0.96 | 0.99 | 0.99 | 0.97 | 0.89 | 0.45 | 0.45 |
| | 0.01 | 0.01 | 0.01 | 0.01 | 0.03 | 0.02 | 0.00 | 0.00 | 0.01 | 0.06 | 0.47 | 0.47 |
| **Overall Mean** | 0.95 | 0.95 | 0.95 | 0.92 | 0.91 | 0.91 | 0.94 | 0.93 | 0.93 | 0.92 | 0.58 | 0.63 |
| **SD** | 0.07 | 0.03 | 0.07 | 0.12 | 0.08 | 0.06 | 0.11 | 0.17 | 0.14 | 0.13 | 0.23 | 0.24 |
| **CV** | 0.08 | 0.03 | 0.07 | 0.13 | 0.09 | 0.07 | 0.12 | 0.18 | 0.15 | 0.14 | 0.40 | 0.38 |

TABLE 4 Nei's diversity and mean values for 12 quantitative traits of *Parastagonospora nodorum*.

| **Population** | Nei's Diversity | Growth Rate 24°C (control) | Growth Rate 18°C | Growth Rate 30°C | Growth Rate 0.1 ppm | Growth Rate 0.5 ppm | Growth Rate 1 ppm | Grey Value 24°C (control) | Grey Value 18°C | Grey Value 30°C | Grey Value 0.1 ppm | Grey Value 0.5 ppm | Grey Value 1 ppm |
|---|---|---|---|---|---|---|---|---|---|---|---|---|---|
| **Australia** | 0.091E* | 4.37B | 3.63B | 2.48A | 2.57CDE | 0.96C | 0.59C | 70.40C | 81.73B | 51.40C | 66.01BC | 50.88C | 56.79B |
| **South Africa** | 0.095DE | 4.86AB | 3.94AB | 1.93B | 2.52DE | 1.01C | 0.58C | 80.64ABC | 89.87AB | 59.43ABC | 82.19AB | 71.85ABC | 85.30A |
| **Switzerland** | 0.120B | 5.26A | 4.26A | 2.52A | 4.33A | 2.66B | 1.88B | 79.74BC | 89.40AB | 57.98BC | 85.01AB | 72.11AB | 67.78AB |
| **China** | 0.121B | 5.11A | 4.20A | 2.56A | 4.66A | 3.27A | 2.38A | 71.81C | 82.28B | 50.57C | 73.35ABC | 64.19ABC | 59.88B |
| **Iran** | 0.131A | 5.37A | 4.28A | 2.62A | 2.97BC | 1.09C | 0.65C | 94.56AB | 100.05A | 77.31A | 75.29ABC | 69.38ABC | 64.42AB |
| **New York** | 0.100CD | 5.25A | 4.37A | 2.49A | 2.83BCD | 0.86C | 0.51C | 93.37AB | 103.55A | 72.63AB | 84.46AB | 73.26AB | 74.82AB |
| **Oregon** | 0.105C | 5.11A | 4.19A | 2.57A | 2.38E | 0.65C | 0.48C | 97.43A | 97.86AB | 74.11AB | 90.80A | 77.70A | 75.04AB |
| **Texas** | 0.102C | 5.17A | 4.20A | 2.70A | 3.12B | 0.97C | 0.53C | 69.79C | 82.21B | 47.24C | 56.96C | 51.95BC | 60.61B |
| **Overall Mean** | 0.11 | 5.06 | 4.13 | 2.48 | 3.17 | 1.44 | 0.95 | 82.22 | 90.87 | 61.33 | 76.76 | 66.42 | 68.08 |
| **SD** | 0.01 | 0.32 | 0.24 | 0.24 | 0.86 | 0.97 | 0.74 | 11.46 | 8.70 | 11.80 | 11.18 | 10.00 | 9.67 |

*Values followed by different letters in the same column are significantly different at $P \leq 0.05$.

TABLE 5 Estimated pairwise $F_{ST}$ according to Nei (1987) based on 49429 neutral SNPs from 164 isolates of *Parastagonospora nodorum*.

| | Australia | South Africa | Switzerland | China | Iran | New York | Oregon | Texas |
|---|---|---|---|---|---|---|---|---|
| Australia | | 0.16 | 0.13 | 0.12 | 0.24 | 0.17 | 0.15 | 0.18 |
| South Africa | | | 0.15 | 0.15 | 0.22 | 0.20 | 0.19 | 0.20 |
| Switzerland | | | | 0.00 | 0.15 | 0.08 | 0.06 | 0.08 |
| China | | | | | 0.15 | 0.08 | 0.06 | 0.08 |
| Iran | | | | | | 0.20 | 0.20 | 0.20 |
| New York | | | | | | | 0.08 | 0.04 |
| Oregon | | | | | | | | 0.08 |
| Texas | | | | | | | | |

## References


Alizon, S., Hurford, A., Mideo, N., & Baalen, M. V. (2009). Virulence evolution and the trade-off hypothesis: history, current state of affairs and the future. *Journal of Evolutionary Biology*, *22*(2), 245–259. doi: 10.1111/j.1420-9101.2008.01658.x

Angilletta, M., Oufiero, C. E., & Leaché, A. D. (2006). Direct and Indirect Effects of Environmental Temperature on the Evolution of Reproductive Strategies: An Information-Theoretic Approach. *The American Naturalist*, *168*(4), E123–E135. doi: 10.1086/507880

Bates, D., Mächler, M., Bolker, B., & Walker, S. (2015). Fitting Linear Mixed-Effects Models Using lme4. *Journal of Statistical Software*, *67*(1). doi: 10.18637/jss.v067.i01

Blixt, E., Olson, Å., Lindahl, B., Djurle, A., & Yuen, J. (2010). Spatiotemporal variation in the fungal community associated with wheat leaves showing symptoms similar to stagonospora nodorum blotch. *European Journal of Plant Pathology*, *126*(3), 373–386. doi: 10.1007/s10658-009-9542-z

Bolger, A., Lohse, M., & Usadel, B. (2014). Trimmomatic: a flexible trimmer for Illumina sequence data. *Bioinformatics*, *30*(15). doi: 10.1093/bioinformatics/btu170

Boots, M., Hudson, P. J., & Sasaki, A. (2004). Large Shifts in Pathogen Virulence Relate to Host Population Structure. *Science*, *303*(5659), 842–844. doi: 10.1126/science.1088542

Bridelli, M. G., Ciati, A., & Crippa, P. R. (2006). Binding of chemicals to melanins re-examined: Adsorption of some drugs to the surface of melanin particles. *Biophysical Chemistry*, *119*(2), 137–145. doi: 10.1016/j.bpc.2005.06.004

Brunner, P. C., Stefanato, F. L., & McDonald, B. A. (2008). Evolution of the *CYP51* gene in *Mycosphaerella graminicola*: evidence for intragenic recombination and selective replacement. *Molecular Plant Pathology*, *9*(3), 305–316. doi: 10.1111/j.1364-3703.2007.00464.x

Butler, M., & Day, A. (1998). Fungal melanins: a review. *Canadian Journal of Microbiology*, *44*(12), 1115–1136. doi: 10.1139/w98-119

Calvo, A. M., Wilson, R. A., Bok, J., & Keller, N. P. (2002). Relationship between Secondary Metabolism and Fungal Development. *Microbiology and Molecular Biology Reviews*, *66*(3), 447–459. doi: 10.1128/mmbr.66.3.447-459.2002

Chang, C. C., Chow, C. C., Tellier, L., Vattikuti, S., Purcell, S. M., & Lee, J. J. (2015). Second-generation PLINK: rising to the challenge of larger and richer datasets. *GigaScience*, *4*(1), 1–16. doi: 10.1186/s13742-015-0047-8

Chevin, L.-M., Lande, R., & Mace, G. M. (2010). Adaptation, Plasticity, and Extinction in a Changing Environment: Towards a Predictive Theory. *PLoS Biology*, *8*(4), e1000357. doi: 10.1371/journal.pbio.1000357

Choi, Y.-E., & Goodwin, S. B. (2011). Gene encoding a c-type cyclin in *Mycosphaerella graminicola* is involved in aerial mycelium formation, filamentous growth, hyphal swelling, melanin biosynthesis, stress response, and pathogenicity. *Molecular Plant-Microbe Interactions : MPMI*, *24*(4), 469–477. doi: 10.1094/mpmi-04-10-0090

Chumley, F. G., & Valent, B. (1990). Genetic Analysis of Melanin-Deficient, Nonpathogenic Mutants of *Magnaporthe grisea*. *Molecular Plant-Microbe Interactions*, *3*(3), 135. doi: 10.1094/mpmi-3-135

Cooper, B. S., Tharp, J. M., Jernberg, I. I., & Angilletta, M. J. (2012). Developmental plasticity of thermal tolerances in temperate and subtropical populations of *Drosophila*

*melanogaster*. *Journal of Thermal Biology*, *37*(3), 211–216. doi: 10.1016/j.jtherbio.2012.01.001

Cordero, R. J. B., & Casadevall, A. (2017). Functions of fungal melanin beyond virulence. *Fungal Biology Reviews*, *31*(2), 99–112. doi: 10.1016/j.fbr.2016.12.003

Corredor-Moreno, P., & Saunders, D. G. O. (2019). Expecting the unexpected: factors influencing the emergence of fungal and oomycete plant pathogens. *New Phytologist*. doi: 10.1111/nph.16007

Dadachova, E., Bryan, R. A., Huang, X., Moadel, T., Schweitzer, A. D., Aisen, P., … Casadevall, A. (2007). Ionizing Radiation Changes the Electronic Properties of Melanin and Enhances the Growth of Melanized Fungi. *PLoS ONE*, *2*(5), e457. doi: 10.1371/journal.pone.0000457

Dadachova, E., & Casadevall, A. (2008). Ionizing radiation: how fungi cope, adapt, and exploit with the help of melanin. *Current Opinion in Microbiology*, *11*(6), 525–531. doi: 10.1016/j.mib.2008.09.013

Danecek, P., Auton, A., Abecasis, G., Albers, C. A., Banks, E., DePristo, M. A., … Group, 1000. (2011). The variant call format and VCFtools. *Bioinformatics*, *27*(15), 2156–2158. doi: 10.1093/bioinformatics/btr330

Eisenman, H. C., & Casadevall, A. (2012). Synthesis and assembly of fungal melanin. *Applied Microbiology and Biotechnology*, *93*(3), 931–940. doi: 10.1007/s00253-011-3777-2

Elderd, B. D., & Reilly, J. R. (2014). Warmer temperatures increase disease transmission and outbreak intensity in a host–pathogen system. *Journal of Animal Ecology*, *83*(4), 838–849. doi: 10.1111/1365-2656.12180

Falconer, D. S., & Mackay, T. F. (1996). Introduction to quantitative genetics. *Longman*.

Ficke, A., Cowger, C., Bergstrom, G. C., & Brodal, G. (2017). Understanding yield loss and pathogen biology to improve disease management: Septoria nodorum blotch - a case study in wheat. *Plant Disease*. doi: 10.1094/pdis-09-17-1375-fe

Fisher, M. C., Henk, Daniel. A., Briggs, C. J., Brownstein, J. S., Madoff, L. C., McCraw, S. L., & Gurr, S. J. (2012). Emerging fungal threats to animal, plant and ecosystem health. *Nature*, *484*(7393), 186. doi: 10.1038/nature10947

Fones, H., & Gurr, S. (2015). The impact of Septoria tritici Blotch disease on wheat: An EU perspective. *Fungal Genetics and Biology*, *79*, 3–7. doi: 10.1016/j.fgb.2015.04.004

Fox, J. (2005). The *R* Commander: A Basic-Statistics Graphical User Interface to *R*. *Journal of Statistical Software*, *14*(9). doi: 10.18637/jss.v014.i09

Gilbert, J., & Woods, S. M. (2001). Leaf spot diseases of spring wheat in southern Manitoba farm fields under conventional and conservation tillage. *Canadian Journal of Plant Science*, *81*(3), 551–559. doi: 10.4141/p00-088

Goudet, J. (2005). hierfstat, a package for r to compute and test hierarchical F-statistics. *Molecular Ecology Notes*, *5*(1), 184–186. doi: 10.1111/j.1471-8286.2004.00828.x

Hagiwara, D., Sakai, K., Suzuki, S., Umemura, M., Nogawa, T., Kato, N., … Kamei, K. (2017). Temperature during conidiation affects stress tolerance, pigmentation, and trypacidin accumulation in the conidia of the airborne pathogen Aspergillus fumigatus. *PLOS ONE*, *12*(5), e0177050. doi: 10.1371/journal.pone.0177050

Hayden, E. J., Bratulic, S., Koenig, I., Ferrada, E., & Wagner, A. (2014). The Effects of Stabilizing and Directional Selection on Phenotypic and Genotypic Variation in a Population of RNA Enzymes. *Journal of Molecular Evolution*, *78*(2), 101–108. doi: 10.1007/s00239-013-9604-x

Hovmoller, M., Yahyaoui, A., Milus, E., & Justesen, A. (2008). Rapid global spread of two aggressive strains of a wheat rust fungus. *Molecular Ecology*, *17*(17), 3818–3826. doi: 10.1111/j.1365-294x.2008.03886.x

Knies, J. L., & Kingsolver, J. G. (2010). Erroneous Arrhenius: Modified Arrhenius Model Best Explains the Temperature Dependence of Ectotherm Fitness. *The American Naturalist*, *176*(2), 227–233. doi: 10.1086/653662

Knorr, K., Jørgensen, L. N., & Nicolaisen, M. (2019). Fungicides have complex effects on the wheat phyllosphere mycobiome. *PLOS ONE*, *14*(3), e0213176. doi: 10.1371/journal.pone.0213176

Krishnan, P., Meile, L., Plissonneau, C., Ma, X., Hartmann, F., Croll, D., … Sánchez-Vallet, A. (2018). Transposable element insertions shape gene regulation and melanin production in a fungal pathogen of wheat. *BMC Biology*. doi: 10.1186/s12915-018-0543-2

Laine, A. (2008). Temperature-mediated patterns of local adaptation in a natural plant–pathogen metapopulation. *Ecology Letters*, *11*(4), 327–337. doi: 10.1111/j.1461-0248.2007.01146.x

Langmead, B., & Salzberg, S. (2012). Fast gapped-read alignment with Bowtie 2. *Nature Methods*, *9*(4). doi: 10.1038/nmeth.1923

Leinonen, T., McCairns, R. J. S., O'Hara, R. B., & Merilä, J. (2013). QST–FST comparisons: evolutionary and ecological insights from genomic heterogeneity. *Nature Reviews Genetics*, *14*(3), 179. doi: 10.1038/nrg3395

Leinonen, T., O'Hara, R., Cano, J., & Merilä, J. (2008). Comparative studies of quantitative trait and neutral marker divergence: a meta-analysis. *Journal of Evolutionary Biology*, *21*(1), 1–17. doi: 10.1111/j.1420-9101.2007.01445.x

Lendenmann, M. H., Croll, D., & McDonald, B. A. (2015). QTL mapping of fungicide sensitivity reveals novel genes and pleiotropy with melanization in the pathogen *Zymoseptoria tritici*. *Fungal Genetics and Biology*, *80*(Nat. Rev. Microbiol. 3 2005), 53–67. doi: 10.1016/j.fgb.2015.05.001

Lendenmann, M. H., Croll, D., Stewart, E. L., & McDonald, B. A. (2014). Quantitative Trait Locus Mapping of Melanization in the Plant Pathogenic Fungus *Zymoseptoria tritici*. *G3: Genes|Genomes|Genetics*, *4*(12). doi: 10.1534/g3.114.015289

McDonald, B. A., & Stukenbrock, E. H. (2016). Rapid emergence of pathogens in agro-ecosystems: global threats to agricultural sustainability and food security. *Philosophical Transactions of the Royal Society B: Biological Sciences*, *371*(1709), 20160026. doi: 10.1098/rstb.2016.0026

McDonald, M. C., Razavi, M., Friesen, T. L., Brunner, P. C., & McDonald, B. A. (2012). Phylogenetic and population genetic analyses of *Phaeosphaeria nodorum* and its close relatives indicate cryptic species and an origin in the Fertile Crescent. *Fungal Genetics and Biology*, *49*(11). doi: 10.1016/j.fgb.2012.08.001

McDonald, M. C., Renkin, M., Spackman, M., Orchard, B., Croll, D., Solomon, P. S., & Milgate, A. (2018). Rapid parallel evolution of azole fungicide resistance in Australian populations of the wheat pathogen *Zymoseptoria tritici*. *Applied and Environmental Microbiology*. doi: 10.1128/AEM.01908-18

McKenna, A., Hanna, M., Banks, E., Sivachenko, A., Cibulskis, K., Kernytsky, A., … DePristo, M. (2010). The Genome Analysis Toolkit: A MapReduce framework for analyzing next-generation DNA sequencing data. *Genome Research*, *20*(9). doi: 10.1101/gr.107524.110

Merilä, J., & Crnokrak, P. (2001). Comparison of genetic differentiation at marker loci and quantitative traits. *Journal of Evolutionary Biology*, *14*(6), 892–903. doi: 10.1046/j.1420-9101.2001.00348.x

Milus, E. A., Kristensen, K., & Hovmøller, M. S. (2009). Evidence for Increased Aggressiveness in a Recent Widespread Strain of *Puccinia striiformis* f. sp. *tritici* Causing Stripe Rust of Wheat. *Phytopathology*, *99*(1), 89–94. doi: 10.1094/phyto-99-1-0089

Murray, G., & Brennan, J. (2009). Estimating disease losses to the Australian wheat industry. *Australasian Plant Pathology*, *38*(6). doi: 10.1071/AP09053

Nosanchuk, J. D., & Casadevall, A. (2003). The contribution of melanin to microbial pathogenesis. *Cellular Microbiology*, *5*(4), 203–223. doi: 10.1046/j.1462-5814.2003.00268.x

Nosanchuk, J. D., & Casadevall, A. (2006). Impact of Melanin on Microbial Virulence and Clinical Resistance to Antimicrobial Compounds. *Antimicrobial Agents and Chemotherapy*, *50*(11), 3519–3528. doi: 10.1128/aac.00545-06

Oliver, R., Friesen, T., Faris, J., & Solomon, P. (2012). *Stagonospora nodorum*: From Pathology to Genomics and Host Resistance. *Annual Review of Phytopathology*, *50*(1), 23–43. doi: 10.1146/annurev-phyto-081211-173019

Paolo, W. F., Dadachova, E., Mandal, P., Casadevall, A., Szaniszlo, P. J., & Nosanchuk, J. D. (2006). Effects of disrupting the polyketide synthase gene *WdPKS1* in *Wangiella* [Exophiala] *dermatitidis* on melanin production and resistance to killing by antifungal compounds, enzymatic degradation, and extremes in temperature. *BMC Microbiology*, *6*(1), 55. doi: 10.1186/1471-2180-6-55

Pereira, D. A., McDonald, B. A., & Brunner, P. C. (2017). Mutations in the *CYP51* gene reduce DMI sensitivity in *Parastagonospora nodorum* populations in Europe and China. *Pest Management Science*, *73*(7). doi: 10.1002/ps.4486

Pereira, D. A. S., Ceresini, P., Castroagudín, V. L., Molina, L. M. R., Mesa, E. C., Negrisoli, M. M., … Takada, H. M. (2016). Population genetic structure of *Rhizoctonia oryzae-sativae* from rice in Latin America and its adaptive potential to emerge as pathogen on Urochloa pastures. *Phytopathology*, *107*(1), 121–131. doi: 10.1094/phyto-05-16-0219-r

Pfeifer, B., Wittelsbürger, U., Ramos-Onsins, S. E., & Lercher, M. J. (2014). PopGenome: An Efficient Swiss Army Knife for Population Genomic Analyses in R. *Molecular Biology and Evolution*, *31*(7), 1929–1936. doi: 10.1093/molbev/msu136

Price, C. L., Parker, J. E., Warrilow, A. G., Kelly, D. E., & Kelly, S. L. (2015). Azole fungicides – understanding resistance mechanisms in agricultural fungal pathogens. *Pest Management Science*, *71*(8), 1054–1058. doi: 10.1002/ps.4029

Qin, C.-F., He, M.-H., Chen, F.-P., Zhu, W., Yang, L.-N., Wu, E.-J., … Zhan, J. (2016). Comparative analyses of fungicide sensitivity and SSR marker variations indicate a low risk of developing azoxystrobin resistance in *Phytophthora infestans*. *Scientific Reports*, *6*(1), 20483. doi: 10.1038/srep20483

Quaedvlieg, W., Verkley, G. J. M., Shin, H.-D., Barreto, R. W., Alfenas, A. C., Swart, W. J., … Crous, P. W. (2013). Sizing up Septoria. *Studies in Mycology*, *75*(Phytopathology942004), 307–390. doi: 10.3114/sim0017

R Core Team. (2019). *R: A Language and Environment for Statistical Computing*. Retrieved from https://www.R-project.org

Rehnstrom, A. L., & Free, S. J. (1996). The isolation and characterization of melanin-deficient mutants of *Monilinia fructicola*. *Physiological and Molecular Plant Pathology*, *49*(5), 321–330. doi: 10.1006/pmpp.1996.0057

Richards, J. K., Wyatt, N. A., Liu, Z., Faris, J. D., & Friesen, T. L. (2017). Reference Quality Genome Assemblies of Three *Parastagonospora nodorum* Isolates Differing in Virulence on Wheat. *G3: Genes, Genomes, Genetics*, *8*(2), g3.300462.2017. doi: 10.1534/g3.117.300462

Sanjak, J. S., Sidorenko, J., Robinson, M. R., Thornton, K. R., & Visscher, P. M. (2018). Evidence of directional and stabilizing selection in contemporary humans. *Proceedings of the National Academy of Sciences*, *115*(1), 151–156. doi: 10.1073/pnas.1707227114

Savary, S., Willocquet, L., Pethybridge, S., Esker, P., McRoberts, N., & Nelson, A. (2019). The global burden of pathogens and pests on major food crops. *Nature Ecology & Evolution*, *3*(3), 430–439. doi: 10.1038/s41559-018-0793-y

Shaw, M., Bearchell, S., Fitt, B., & Fraaije, B. (2008). Long-term relationships between environment and abundance in wheat of *Phaeosphaeria nodorum* and Mycosphaerella graminicola. *New Phytologist*, *177*(1), 229–238. doi: 10.1111/j.1469-8137.2007.02236.x

Singaravelan, N., Grishkan, I., Beharav, A., Wakamatsu, K., Ito, S., & Nevo, E. (2008). Adaptive Melanin Response of the Soil Fungus *Aspergillus niger* to UV Radiation Stress at "Evolution Canyon", Mount Carmel, Israel. *PLoS ONE*, *3*(8), e2993. doi: 10.1371/journal.pone.0002993

Spitze, K. (1993). Population structure in *Daphnia obtusa*: quantitative genetic and allozymic variation. *Genetics*, *135*(2), 367–374.

Stefansson, T. S., McDonald, B. A., & Willi, Y. (2013). Local adaptation and evolutionary potential along a temperature gradient in the fungal pathogen *Rhynchosporium commune*. *Evolutionary Applications*, *6*(3), 524–534. doi: 10.1111/eva.12039

Stefansson, T., Willi, Y., Croll, D., & McDonald. (2014). An assay for quantitative virulence in *Rhynchosporium commune* reveals an association between effector genotype and virulence. *Plant Pathology*, *63*(2), 405–414. doi: 10.1111/ppa.12111

Stukenbrock, E. H., Banke, S., & McDonald, B. A. (2006). Global migration patterns in the fungal wheat pathogen *Phaeosphaeria nodorum*. *Molecular Ecology*, *15*(10), 2895–2904. doi: 10.1111/j.1365-294x.2006.02986.x

Stukenbrock, Eva H., & McDonald, B. A. (2008). The Origins of Plant Pathogens in Agro-Ecosystems. *Annual Review of Phytopathology*, *46*(1), 75–100. doi: 10.1146/annurev.phyto.010708.154114

Sturm, R. A., & Duffy, D. L. (2012). Human pigmentation genes under environmental selection. *Genome Biology*, *13*(9), 248. doi: 10.1186/gb-2012-13-9-248

Tonsor, S. J., Elnaccash, T. W., & Scheiner, S. M. (2013). Developmental instability is genetically correlated with phenotypic plasticity, constraining heritability, and fitness. *Evolution*, *67*(10), 2923–2935. doi: 10.1111/evo.12175

Wheeler, M. H., & Bell, A. A. (1988). Melanins and Their Importance in Pathogenic Fungi. In *Springer New York* (pp. 338–387). doi: 10.1007/978-1-4612-3730-3_10

Whitlock, M. C. (2008). Evolutionary inference from QST. *Molecular Ecology*, *17*(8), 1885–1896. doi: 10.1111/j.1365-294X.2008.03712.x

Wickham, H. (2009). *Ggplot2: Elegant Graphics for Data Analysis* (2nd ed.). Springer Publishing Company, Incorporated.

Willi, Y., Frank, A., Heinzelmann, R., Kälin, A., Spalinger, L., & Ceresini, P. C. (2011). The adaptive potential of a plant pathogenic fungus, *Rhizoctonia solani* AG-3, under heat and fungicide stress. *Genetica*, *139*(7), 903. doi: 10.1007/s10709-011-9594-9

Yampolsky, L., Schaer, T., & Ebert, D. (2013). Adaptive phenotypic plasticity and local adaptation for temperature tolerance in freshwater zooplankton. *Proceedings of the Royal Society B: Biological Sciences*, *281*(1776), 20132744–20132744. doi: 10.1098/rspb.2013.2744

Yang, L., Zhu, W., Wu, E., Yang, C., Thrall, P. H., Burdon, J. J., … Zhan, J. (2016). Trade-offs and evolution of thermal adaptation in the Irish potato famine pathogen *Phytophthora infestans*. *Molecular Ecology*, *25*(16), 4047–4058. doi: 10.1111/mec.13727

Zearfoss, A., Cowger, C., & Ojiambo, P. (2011). A Degree-Day Model for the Latent Period of Stagonospora nodorum Blotch in Winter Wheat. *Plant Disease*, *95*(5), 561–567. doi: 10.1094/pdis-09-10-0651

Zhan, J., Linde, C. C., Jürgens, T., Merz, U., Steinebrunner, F., & McDonald, B. A. (2005). Variation for neutral markers is correlated with variation for quantitative traits in the plant pathogenic fungus *Mycosphaerella graminicola*. *Molecular Ecology*, *14*(9), 2683–2693. doi: 10.1111/j.1365-294x.2005.02638.x

Zhan, J., & McDonald, B. (2011). Thermal adaptation in the fungal pathogen *Mycosphaerella graminicola*. *Molecular Ecology*, *20*(8). doi: 10.1111/j.1365-294X.2011.05023.x

Zhu, W., Zhan, J., & McDonald, B. A. (2018). Evidence for local adaptation and pleiotropic effects associated with melanization in a plant pathogenic fungus. *Fungal Genetics and Biology*, (Plant Dis. 92 2008). doi: 10.1016/j.fgb.2018.04.002